Fermi National Accelerator Laboratory

FERMILAB-Conf-93/355-E

CDF

A Measurement of the W Mass using Electrons at CDF

David Saltzberg
For the CDF Collaboration

Enrico Fermi Institute, University of Chicago
Chicago, Illinois

Fermi National Accelerator Laboratory
P.O. Box 500, Batavia, Illinois 60510

November 1993

Published Proceedings *9th Topical Workshop on Proton-Antiproton Collider Physics*,
University of Tsukuba, Tsukuba, Japan, October 18-22, 1993

Disclaimer

CDF/PUB/ELECTROWEAK/PUBLIC/2354
FERMILAB-CONF-93/355-E

A Measurement of the W Mass using Electrons at CDF

David Saltzberg
Enrico Fermi Institute, University of Chicago
5640 South Ellis Avenue, Chicago, Illinois, USA

For the CDF collaboration

We present a preliminary measurement of the mass of the W boson using electron data from the 1992-93 collider run at the Fermilab Tevatron. The result is $M_W = 80.47 \pm 0.15$ (stat.) $\pm$ 0.25 (syst.) GeV. Current predictions agree with this value.

1. Introduction

The Standard Model of the electroweak interaction may be used to predict precise relationships among experimentally measurable quantities. Most measurements may be categorized as those involving neutral versus charged current interactions and those at low Q^2 versus $Q^2 \sim (100\ \mathrm{GeV})^2$, where Q^2 denotes the approximate squared momentum transfer characterizing the interaction. Proton-antiproton colliders can probe electroweak charged currents at high Q^2. Specifically, the measurement of the W boson mass provides a test of this portion of the Standard Model.

This paper describes a preliminary measurement of the mass of the W boson using W decays to an electron and a neutrino. The events were taken from 20.0 pb^{-1} of data collected by the CDF experiment during the 1992-93 collider run at the Fermilab Tevatron. The following section describes the analysis technique and the critical detector components. Sections 3 through 6 detail the steps of the analysis. In Section 7, the result is examined in the context of theoretical predictions and previous measurements.

2. Overview of Analysis

A W is produced with some transverse momentum which is balanced by recoiling hadronic particles. The W bosons in the events used in this analysis subsequently decay into an electron and neutrino. Since the neutrino momentum cannot be measured directly, it must be inferred from the energy of the decay electron and the hadronic energy in the event. Since one does not know the energy of the hard scatter from which the W was produced and cannot measure the z-component of the recoiling hadronic energy, one can infer only the transverse components of the momentum of the neutrino. Hence, there is insufficient information to reconstruct the invariant mass of each W on an event-by-event basis. Rather, we construct the *transverse mass* of the W, which is analogous to the invariant mass except that only the components of energy transverse to the beamline are used. Specifically,

$$M_T^2 = (E_T^e + E_T^\nu)^2 - (\mathbf{E_T^e} + \mathbf{E_T^\nu})^2, \tag{1}$$

where M_T is the transverse mass of the W, E_T^e and E_T^ν are the transverse momenta of the electron and neutrino respectively and boldface denotes two-component vector quantities.

Pub. Proceedings 9th Topical Workshop on Proton-Antiproton Collider Physics, University of Tsukuba, Tsukuba, Japan, October 18-22, 1993.

The transverse mass lineshape is compared to simulated lineshapes for a range of W masses to extract the mass of the W.

The electrons used to measure the W mass at CDF pass through two complementary detectors. Initially, an electron's momentum is measured from the curvature and polar angle of the track left in the central tracking chamber (CTC) as it traverses a 14 kG axial magnetic field parallel to the beamline.[1] After leaving the tracking volume, the electron energy is measured from the size of the shower it produces in the central electromagnetic calorimeter (CEM) which is a lead and plastic scintillator sampling calorimeter.[2] Each of these measurements is independent and limited by different systematics so one device is used to reduce the deficiencies of the other. The advantages of the CTC relative to the CEM are linearity and uniformity. Its disadvantages relative to the CEM are poorer resolution, lack of robustness in measuring the momentum of electrons which emit bremsstrahlung before entering the tracking volume, and false curvatures which cause charge-dependent curvature offsets. Conversely, while the CEM response is non-uniform and non-linear, it has better resolution than the CTC and is robust against biases due to bremsstrahlung radiation, which is mostly collinear with the electron direction. Also, the CEM response to electrons is independent of their charge.

Several data samples are used to calibrate the CTC and CEM responses. Searching for variations with geometry and momentum in the $\psi \rightarrow \mu\ \mu$ mass sets limits on the non-uniformity and non-linearity of the CTC momentum measurement. The CEM has significant time-dependences, edge effects, and variations in gain from tower to tower. A large sample of approximately 150,000 inclusive electrons with $E_T > 9$ GeV exploits the stability and uniformity of the CTC measurement to correct the response of the CEM by requiring that the ratio of the CEM energy measurement to the CTC momentum measurement (E/P) be independent of time and shower position. The final calibration will be made with a sample over twice this size. A sample of electrons with $E_T > 18$ GeV provides a sample of tracks sensitive to false curvatures in the CTC measurement. Since the CEM measurement is charge-independent, constraining the ratio E/P to have the same mean for positive and negative electrons removes false curvatures in the CTC.

The absolute energy scale of the CEM is determined from the absolute momentum scale of the CTC. This method gives a better final uncertainty than normalizing to the Z mass because of the limited number of $Z \rightarrow e\ e$ events. In the following section, we set the absolute scale of the CTC by normalizing the ψ mass peak to the world-average mass value. In Section 4, the CEM energy scale is determined from the CTC momentum scale by normalizing the measured E/P ratio for electrons from W events to a radiative simulation. In Section 5, the measurement of the energy recoiling against the W transverse momentum is calibrated. Section 6 describes how the W mass is extracted from the observed transverse mass spectrum.

3. CTC Momentum Scale

The CTC momentum scale will determine the energy scale of the CEM which, in turn, is used to measure the W mass. The mean of the approximately 60,000 $\psi \rightarrow \mu\ \mu$ events

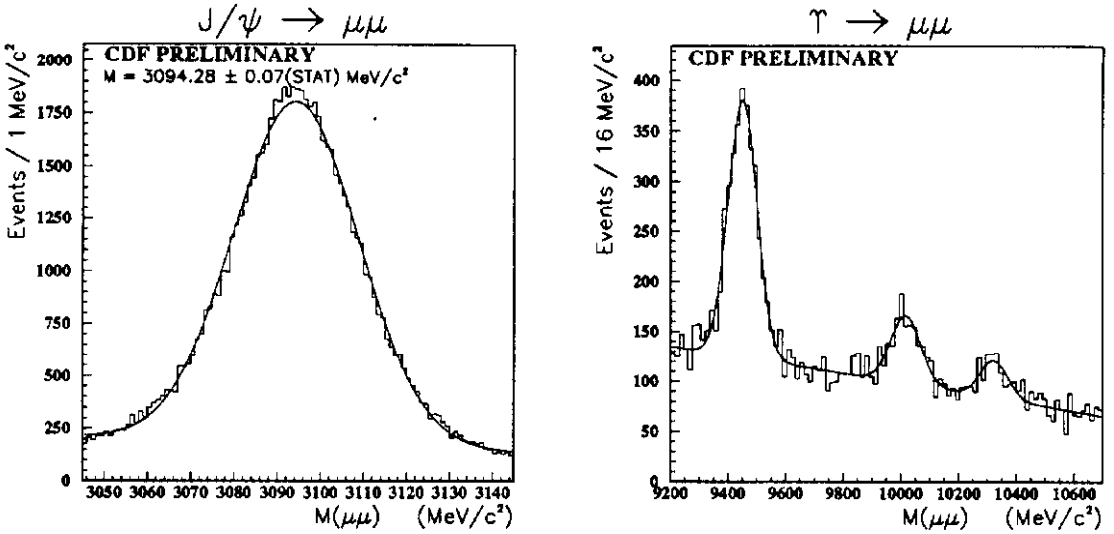

Figure 1: Dimuon mass spectrum near the ψ mass (left). Dimuon mass spectrum near the Υ mass (right).

above background shown in Figure 1 will be normalized to the Particle Data Group's value of 3096.9 MeV[3] to set the CTC momentum scale. As a check, after all CTC corrections, we measure the masses of the $\Upsilon(1S)$, $\Upsilon(2S)$ and $\Upsilon(3S)$. There are approximately 2000 events above background in these peaks which are shown in Figure 1.

A list of systematic errors in measuring the ψ mass and in extrapolating to the curvatures of W electrons is given in Table 1. Even though many of these effects are likely to be correlated, uncertainties are treated as if independent to obtain a conservative estimate of the total systematic error. We now discuss each item on the list. The data are fit to a Gaussian with a linear background. The mean is determined to 0.1 MeV and is independent of the fit window. Each muon is corrected for minimum-ionizing energy loss in material traversed before entering the tracking volume. The amount of material is calculated both from a detailed accounting of all matter installed between the beamline and tracking volume and is also directly measured from the size of the radiative tail of the E/P distribution for W electrons. The radiative measurement indicates 30% more material than indicated from the accounting so a shift of $+1.0 \pm 1.0$ MeV is applied to the measured ψ mass. The mass shifts by 0.5 MeV when the tracks are constrained to originate from the event vertex; the shift is taken as a systematic error. A dependence of the ψ mass on the opening polar angle between the two tracks is observed. Since there is no polar angle difference to take in W events, the difference between the average ψ mass and those which have tracks back-to-back in polar angle (and hence have no mass dependence on the difference) is taken as a shift of -1.0 ± 1.0 MeV. Even after the measured magnetic field map is included in the fits, a residual mass dependence on the two tracks' trajectories through the solenoidal field is observed and contributes an additional 1.1 MeV uncertainty. Breaking up the dataset into smaller samples and comparing the mass shifts between linear and quadratic background shapes shows

Statistics	0.1 MeV
Muon energy loss before tracking	1.0 MeV
Vertex-constraint	0.5 MeV
Opening polar angle effect	1.0 MeV
Residual field non-uniformity	1.1 MeV
Background	0.1 MeV
Time Variation	1.0 MeV
Radiative Decay	0.3 MeV
Non-linearity	0.5 MeV
TOTAL	2.2 MeV

Table 1: Summary of uncertainties incurred using the ψ peak to set the CTC scale for tracks from W electrons. A 2.2 MeV uncertainty on the ψ mass corresponds to a 60 MeV uncertainty on the W mass.

that the presence of background adds an additional 0.1 MeV uncertainty. An unexplained time-dependence in the ψ mass has been observed; the shift over the span of the run used in the analysis, 1.0 MeV, is taken as a systematic error. The shift due to radiative decays of the ψ, *i.e.* $\psi \rightarrow \mu\mu\gamma$, is estimated from theory to be 0.3 MeV; we take a $+0.3\pm0.3$ MeV shift. Non-linearities may arise from many of the above systematics or from the limitation of averaging out false curvatures over charge. Studying the ψ events produced in different p_T regions, we estimate the non-linearity could cause as much as a 0.5 MeV shift at the curvatures typical for tracks of W electrons. However, since the effect may have already been corrected by some of the previous shifts and it is small (<15 MeV at the W mass), it is taken as an uncertainty with no corresponding shift. The net systematic uncertainty on the CTC scale for measuring the W mass using the ψ peak as the calibration point is 2.2 MeV when expressed as an uncertainty on the ψ mass or 60 MeV at the W mass. Work is still in progress to understand better the energy-loss correction and the nominal value of the magnetic field.

These corrections and uncertainties are applied to the three observable upsilon peaks as a check. The measured values before and after all scale corrections are shown in Table 2 alongside the Particle Data Group's values.

4. CEM Energy Scale

With the absolute CTC scale in hand, we proceed to set the CEM scale using electrons from $W \rightarrow e\nu$ decays. First, we describe the event selection. Second, we describe the radiative simulation which produces the templates used for fitting the E/P lineshape and determining the CEM scale. Third, the mass of the Z boson is measured as a check.

The first level of trigger requires that at least one CEM calorimeter tower has at least 6 GeV of transverse energy. At the second level trigger, the event must either pass a 9 GeV

CDF PRELIMINARY

	RAW (MeV)	CORRECTED (MeV)	PDG (MeV)
$\Upsilon(1S)$	9449.8 ± 1.8	$9457.0 \pm 1.8 \pm 7$	9460.3 ± 0.2
$\Upsilon(2S)$	10018.0 ± 5	$10026 \pm 5 \pm 7$	10023.3 ± 0.3
$\Upsilon(3S)$	10323 ± 8	$10331 \pm 8 \pm 7$	10355.3 ± 0.5

Table 2: Raw and corrected mass values for Υ peaks compared to the Particle Data Group masses. The first uncertainty on the corrected value is statistical. The second is the systematic error from setting the momentum scale.

inclusive electron trigger or a trigger requiring 20 GeV missing transverse energy and a CEM cluster with transverse energy above 16 GeV with less than 1/8 of its energy in the hadronic compartment. The combination of these triggers is measured to be better than 99.9% efficient for events passing the offline cuts. Similar triggers are used by the third-level (software) trigger. The data are only used if taken during a "good-run" and a run taken during stable running conditions, *i.e.*, not immediately after a long access into the collision hall. These cuts remove 10% of the data recorded to tape, leaving a dataset of 20.0 pb^{-1}. The event must have an electron with high transverse energy, $E_T > 25$ GeV, high missing transverse energy, $\not\!\!E_T > 25$ GeV, and a high transverse mass, $60 < M_T < 100$ GeV. These cuts remove background while retaining most mass information. Events containing jets with $E_T > 20$ GeV are rejected to reduce background and improve the transverse mass resolution. A narrow track isolation cut imposed on the electron removes background without excessively biasing the average flow of hadronic energy in the events. No cuts on the profile of the shower at shower-maximum is made to avoid biasing the selection against electrons which emit bremsstrahlung. Finally, tight fiducial cuts are imposed on the electron to avoid regions of the calorimeter near cracks. After these cuts, 6508 events remain in the data sample.

The ratio of E/P for this sample is shown in Figure 2. The left-hand side of the curve is well described by a Gaussian over three orders of magnitude as one would expect since the ratio is the product of two quantities with roughly Gaussian resolutions. The right-hand side of the curve has a long tail due to internal and external bremsstrahlung emitted by the electron before entering the tracking volume. Since the photon is nearly collinear with the electron, the CEM measurement of E is unaffected by the occurrence of bremsstrahlung but the CTC measurement of P is lowered causing a high-side tail to E/P. The solid histogram is from a radiative Monte Carlo which includes both internal and external radiation of photons. The curvature resolution of the CTC is modelled as:

$$\frac{\delta C}{C} = const., \tag{2}$$

where the constant is floated in the fit to the E/P peak and is found to be consistent with other measurements of this resolution. The electron energy resolution is modelled using:

$$(\frac{\delta E}{E})^2 = (13.5\%\sqrt{E_T})^2 + (const.)^2, \tag{3}$$

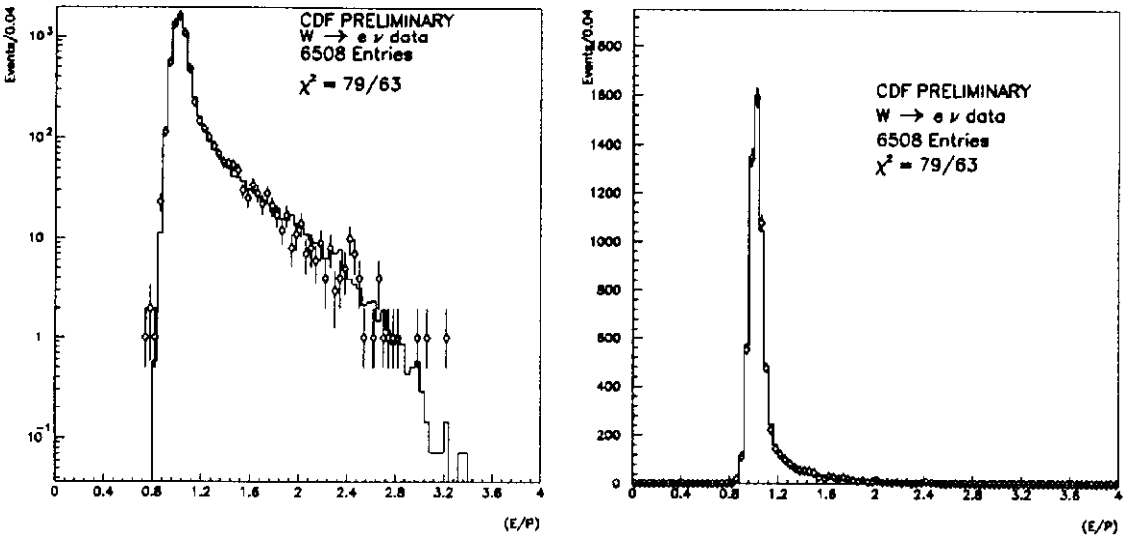

Figure 2: Ratio of the CEM measurement of electron energy (E) to its momentum (P) for the $W \rightarrow e\nu$ sample on both logarithmic (left) and linear (right) scales. The points are the data and the histogram is the radiative simulation.

where the constant term is constrained using the observed width of the $Z \rightarrow e\ e$ peak to be $(2.1 \pm 1.0)\%$. The number of events in the tail of E/P from 1.3 to 2.0 is used to measure the average number of radiation lengths (X_0) traversed by the electrons before entering the tracking volume. This number (approximately 0.087 X_0) is 30% higher than the direct accounting of the material predicts. The CEM scale is measured with a statistical precision of 0.08% and a systematic uncertainty of 0.13%.

A Z sample of 293 events is chosen with both electrons in the central and similar cuts to those used in selecting the W sample. A simulation including contributions from the Drell-Yan continuum and internal bremsstrahlung is used to make predicted observed lineshapes. The best fit lineshape is shown with the data in Figure 3. A correction is made for the 0.00025 ± 0.00015 GeV^{-1} non-linearity of the CEM since the scale was calibrated using W events, not Z events. The best fit is 90.87 ± 0.20 (stat.)± 0.16 (syst.) GeV, which may be compared with the LEP result of 91.187 ± 0.007 GeV. [4]

5. Underlying Event Modelling

A fast leading-order W generator makes W events using the MRSD-' structure functions. The bosons are given transverse momentum with a subsequent boost. To model the transverse mass spectrum, one must calibrate the response of the detector to the hadrons recoiling against the transverse momentum of the W. The measurement of this transverse hadronic flow is a vector quantity which we call **u**. This vector is conveniently discussed as two quantities, $u_{//}$ and $u_{\perp}$ which are its components parallel and perpendicular to the electron direction. This decomposition is useful since $u_{//}$ contains most of the transverse mass information and it is the quantity which can suffer offsets from the electron quality

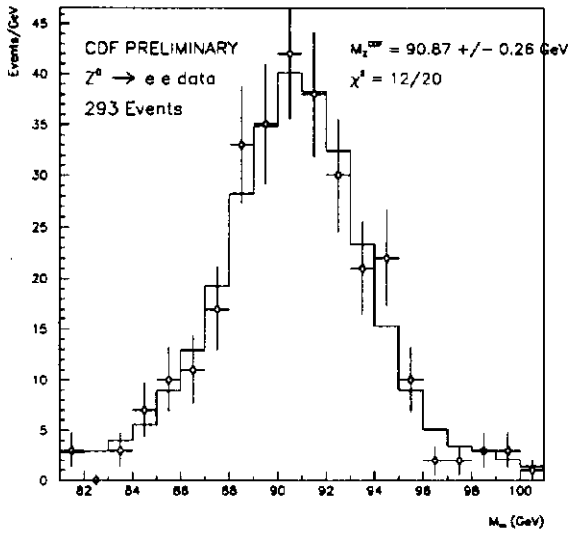

Figure 3: Best fit (histogram) to the Z data (points). The mass value returned is used as a check only.

cuts made in the event selection. The sample used to measure the mass is exactly the same sample as used to measure the CEM energy scale except for an additional requirement that the magnitude of **u** be less than 20 GeV, which leaves 6421 events. In this section, we describe how the response to these low energy hadrons is modelled and show how well the model describes the data.

The response of the detector to the low-energy hadrons recoiling against the W is poorly known. Fortunately, Z bosons are produced at the Tevatron with a similar transverse momentum spectrum as W bosons. Since both leptons from Z decays to charged leptons can be detected we will make use of the fact that the leptons are measured with much better resolution than the recoil to study the response of the detector to the recoil. Specifically, when the W simulation generates a W with a given transverse momentum, the recoil **u** measured from a Z event with the same transverse momentum is used as the underlying event. There are 1194 Z decays to electrons or muons used. The advantage of this method is that there are no detector resolutions which must be tuned to the data. Only the input transverse momentum spectrum given to the generated W events must be tuned. Note that this method of modelling the detector resolution does *not* require that the transverse momentum spectra of the two bosons be the same, only that the possible responses of the detector to a W of given transverse momentum be the same as those from a Z of the same transverse momentum. Currently, we do use the directly observed shape of the Z transverse momentum spectrum after the jet cut as the input shape of the W transverse momentum spectrum. This is scaled by a constant, 1.00 ± 0.05 to give the best fit to the width of the $u_{//}$ and $u_{\perp}$ distributions. The uncertainty covers the range of how hard or soft the spectrum can be made before a 1σ disagreement with the observed spread of the $u_{//}$ and $u_{\perp}$ distributions is observed. The

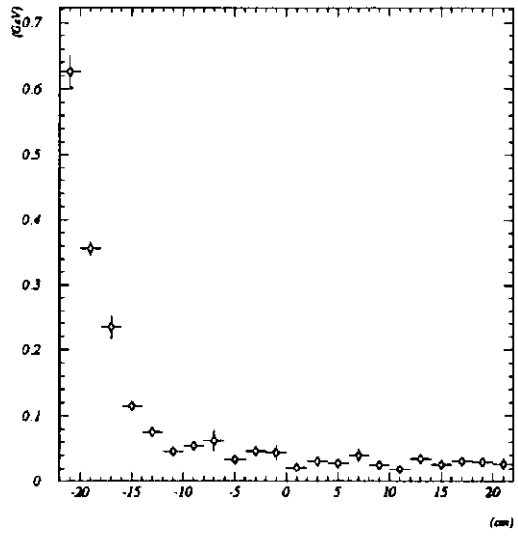

Figure 4: Transverse energy in calorimeter towers adjacent to the electron cluster as a function of the position of the shower. The baseline value of 30 MeV is the amount of transverse energy added back to $u_{//}$ to account for energy flow hidden in the electron cluster.

corresponding uncertainty on the W mass is included in the uncertainty attributed to modelling. As a check, the ability to model the observed $u_{//}$ and $u_{\perp}$ distributions is shown to be unaffected by tightening the cut on the magnitude of **u**.

Selecting events by cutting on electron E_T will induce a bias on $u_{//}$ because decays where the electron is emitted parallel to the W transverse momentum direction are preferentially kept. Figure 4 shows the average transverse energy in the towers adjacent to the electron cluster as a function of the shower position. This energy is the sum of leakage out of the electron cluster and the average transverse energy flow near the electron. We add 30 MeV of $u_{//}$ add per electron tower (typically three towers) to replace the average hadronic energy hidden in the electron cluster. Figure 5 shows that the bias on $u_{//}$ in the data is well modelled by the simulation over the range of electron E_T used in the measurement. Similar agreement is seen versus the transverse energy of the neutrino. The distributions of $u_{\perp}$ and $u_{//}$ are shown in Figures 6. Note that these distributions are non-Gaussian, yet well described by the simulation. The measured offset in $u_{//}$ in the dataset is -405 ± 65 MeV where the predicted offset in $u_{//}$ is -330 MeV. Although the difference is not statistically significant, the difference is taken as a systematic uncertainty. Note that the discrepancy is in the direction expected for a bias due to electron selection cuts. For completeness, the data and prediction for the bias in $u_{//}$ as a function of the magnitude of **u** is shown in Figure 7.

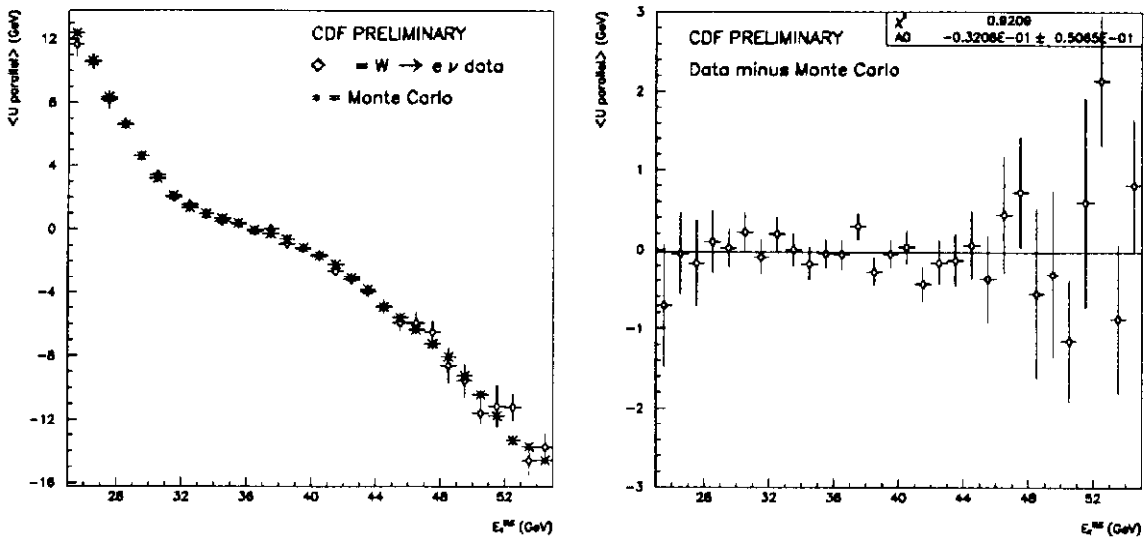

Figure 5: Data (diamonds) versus predicted (asterisks) value of mean offset in $u_{//}$ as a function of the electron E_T in the event (left). The residuals of the data minus the simulation are also shown (right).

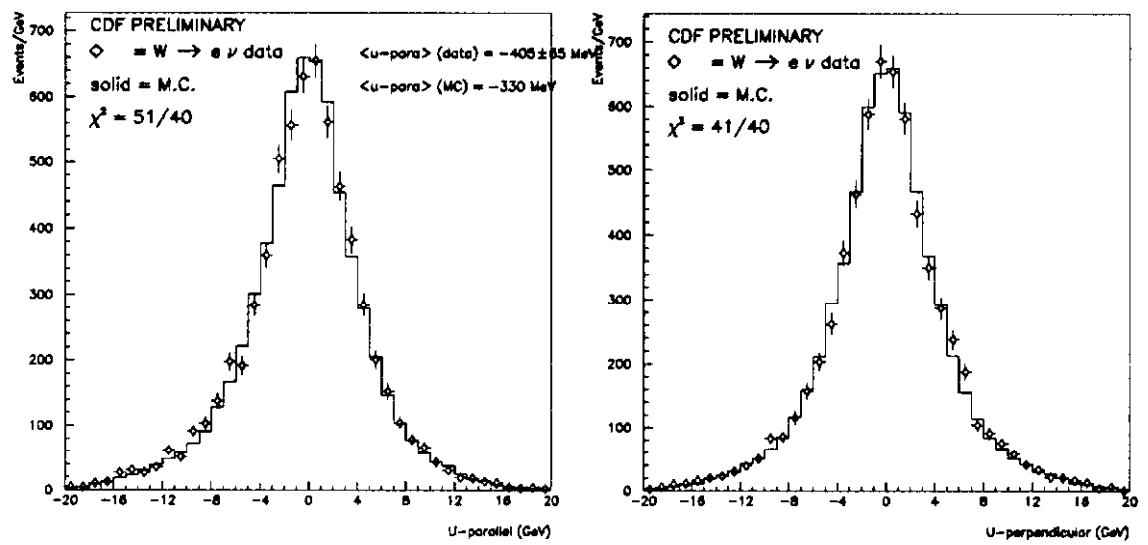

Figure 6: Data (points) versus predicted (histogram) distribution of $u_{//}$ for the W dataset (left). Data (points) versus predicted (histogram) distribution of $u_{\perp}$ for the W dataset (right).

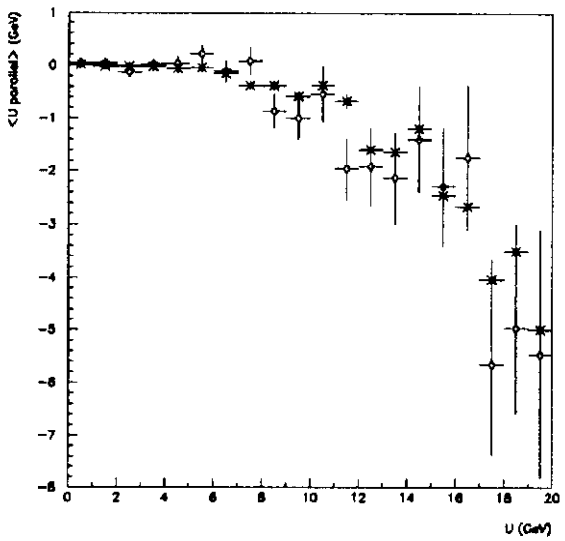

Figure 7: Data (diamonds) versus predicted (asterisks) mean offset of $u_{//}$ as a function of the magnitude of **u**.

6. Fitting for the Mass

Transverse mass spectra are generated from M_T=60 to 100 GeV for a range of W masses 100 MeV apart and a range of W widths 200 MeV apart. The data are compared to each template and a log-likelihood is calculated. The log-likelihood points are fit to a paraboloid. The paraboloid's maximum value occurs at the most likely mass and width combination. As a check, many simulated data samples the same size as the true dataset are fit. The returned masses and widths center on the value at which they were generated with an RMS spread equal to the mean returned statistical error.

The fit to the data with the mass and width floating returns a width consistent with the Standard Model prediction. When the width is fixed at 2.1 GeV, the best value for the W mass shifts by only 10 MeV and the value is:

$$M_W = 80.47 \pm 0.15(\text{stat.}) \pm 0.25(\text{syst.})\ \text{GeV}. \tag{4}$$

The transverse mass spectrum from the data used to fit the W mass and the best-fit lineshape are shown in Figure 8. Using the best-fit mass from the transverse mass fits, the data and prediction of the lepton E_T spectrum are compared in Figure 9. Fits to the individual lepton E_T spectra yield consistent results for the mass.

A summary of the experimental uncertainties in this preliminary analysis are compared to the final uncertainties of the previous run's electron data [5] in Table 3. The largest systematic error of 140 MeV arises from shifts in the mass as the constant term parametrizing the electron resolution is varied within the bounds set by the observed width of the Z peak. The 100 MeV error ascribed to theory bounds the variation in the mass among structure function sets recently considered acceptable.

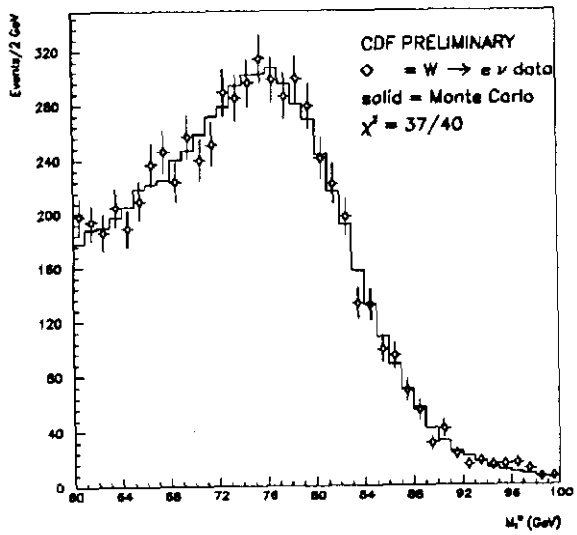

Figure 8: Transverse mass spectrum from the data (points) and best-fit (solid).

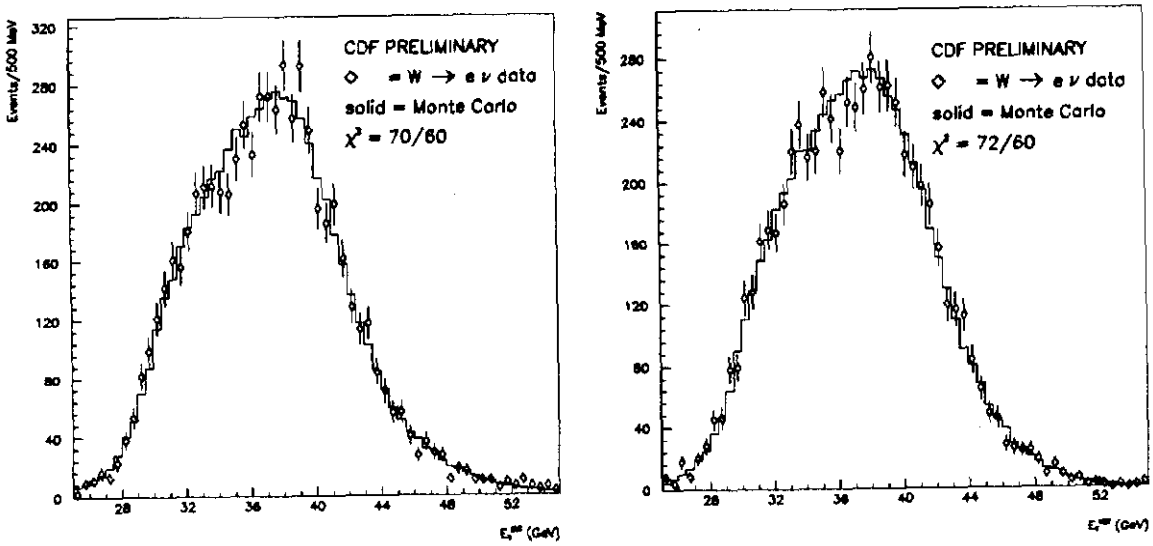

Figure 9: Transverse energy spectra of electron and missing energy compared to the prediction from the best fit to the transverse mass spectrum. The points are the data and the histogram is the simulation.

Quantity	1990	1993
I. Statistical	350 MeV	150 MeV
II. Energy Scale	190 MeV	130 MeV
1. Tracking Chamber	80 MeV	60 MeV
2. Calorimeter	175 MeV	120 MeV
a. Stat error on E/P		64 MeV
b. Syst error on E/P		100 MeV
III. Systematics	230 MeV	190 MeV
1. Electron Resolution	70 MeV	140 MeV
2. Modelling, P_T^W	130 MeV	90 MeV
3. Parallel Balance	170 MeV	70 MeV
4. Background	50 MeV	50 MeV
5. Fitting	50 MeV	20 MeV
IV. Theory	60 MeV	100 MeV
1. Proton Structure	60 MeV	100 MeV
TOTAL UNCERTAINTY	465 MeV	290 MeV

Table 3: Preliminary electron W Mass analysis uncertainties compared to the corresponding final uncertainties in the analysis of the previous run's electron data.

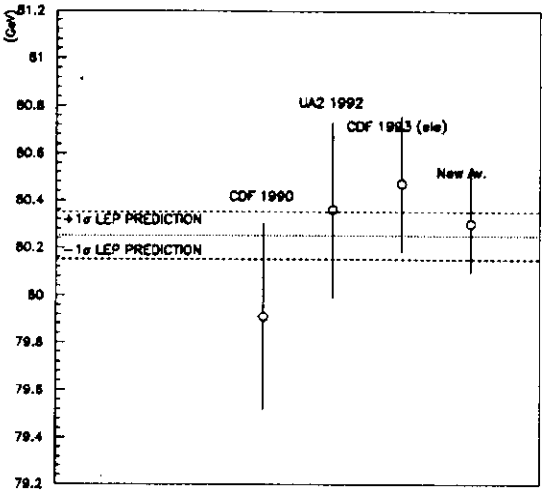

Figure 10: The current measurement of the W mass is compared to recent previous measurements and the Standard Model prediction based on LEP data.

7. Conclusion

In Figure 10, we compare this measurement to recent previous measurements by the CDF[5] and UA2[6] experiments. The new world average[7], 80.30 $\pm$0.20 GeV, is compared to the prediction of 80.25 $\pm$ 0.10 GeV made from the LEP measurements.[4] A difference between the prediction for the W mass and the directly measured value would indicate the presence of physical effects outside the Standard Model. The current measurements indicate no such deviation.

References

[1] F. Bedeschi *et al.*, Nucl. Instr. and Meth., A268 (1988) 50.

[2] L. Balka *et al.*, Nucl. Instr. and Meth., A267 (1988) 272.

[3] M. Aguilar-Benitez *et al.*, *Review of Particle Properties* from Phys. Rev. **D45**, (1992).

[4] M. Swartz, "High Energy Tests of the Electroweak Standard Model", XVI International Symposium on Lepton-Photon Interactions, 10-15 August 1993.

[5] F. Abe *et al.* (CDF Collaboration), Phys. Rev. Lett., **65**, 2243 (1990).

[6] J. Aletti *et al.* (UA2 Collaboration), Phys. Lett. **B276**, 354 (1992). The W mass is calculated using the latest Z mass.

[7] At this conference, Q. Zhu (D0 Collaboration) presented a measurement of the W mass of 79.86$\pm$0.40 GeV. The new world average including this measurement is 80.21$\pm$0.18 GeV.